

Hypericin-Induced Cell Photosensitization Involves an Intracellular pH Decrease

F. Sureau,^{*,†} P. Miskovsky,[‡] L. Chinsky,[†] and P. Y. Turpin[†]

Contribution from the L.P.B.C. (CNRS URA 2056), Université P. et M. Curie, Case 138, 4 Place Jussieu, 75231 Paris Cedex 05, France, and Biophysics Division, Safarik University, Jesenna 5, 04154 Kosice, Slovakia

Received May 28, 1996[⊗]

Abstract: Snarf-1-AM (Seminaphthorhodafuor-1-acetoxymethylester) being used as a fluorescent pH probe, confocal laser microspectrofluorometric measurements allowed intracellular pH to be assessed within 3T3 mouse fibroblasts in the presence or in the absence of hypericin. Cytoplasmic local pH drops of 0.4 unit have been measured in the presence of 1 μ M hypericin after 90 s of exposure to 0.1 μ W of illumination at 514 nm. Moreover, time course experiments clearly show that this local pH decrease is actually light dose dependent. Taking into account previously reported results and interpretations, it is shown here that this pH decrease has to be considered as one of the possible processes responsible for the photosensitizing properties of hypericin, involved in its virucidal and antitumor activities.

Introduction

Hypericin (Figure 1) is a natural photosensitizing polycyclic aromatic dione, which can be extracted from plants of the *Hypericum* genus¹ and corresponds to the parent chromophore of the stentorin photoreceptor isolated from *Stentor coeruleus*.² It displays virucidal activity against several types of viruses, including the Human immunodeficiency virus (HIV),^{3–6} as well as antiproliferative and cytotoxic effects on tumor cells.^{7–9} Its virucidal activity is enhanced more than 100-fold in the presence of light:^{3,6,10} this has been reported to be related to the inhibition of reverse transcriptase activity of mature virion.¹¹ Other biological properties have also been described, such as potent antidepressive activity,¹² light-dependent inhibition of protein kinase C (PKC),^{7,13} photoinduced inhibition of epidermal growth factor (EGF) receptor, tyrosine kinase activity,¹⁴ and photosensitized inhibition of mitochondrial succinoxidase.¹⁵ Hypericin,

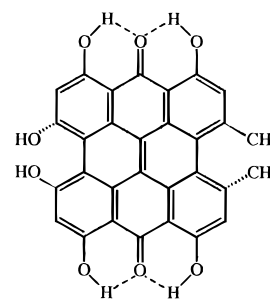


Figure 1. Structure of hypericin.

like many other anticancer drugs, has also been reported to induce apoptosis.⁹

In view of the photobiological relevancy, excited state properties of hypericin have been widely studied, in order to understand the role of light on its biological activity.^{16–21} Nevertheless its mechanism and site of action at the cellular level still remain unclear,²² and various photophysical processes have been proposed to account for its photosensitizing properties:

(i) An oxygen-dependent mechanism has first been reported^{3,6} since irradiation of hypericin with visible light leads to the production of singlet oxygen (¹O₂) with a yield of ≈ 0.35 when embedded in DPPC (dipalmitoylphosphatidylcholine) liposomes.¹⁶ The formation of singlet oxygen as a primary oxidizer occurs via energy transfer from the excited triplet state of hypericin towards the ground state of molecular oxygen.^{24,25} However, although this type II oxygen-dependent photosensi-

[†] Université P. et M. Curie.

[‡] Safarik University.

[⊗] Abstract published in *Advance ACS Abstracts*, September 15, 1996.

(1) Duran, N.; Song, P. S. *Photochem. Photobiol.* **1986**, *48*, 667–680.
(2) Walker, E. B.; Lee, T. Y.; Song, P. S. *Biochim. Biophys. Acta* **1979**, *587*, 129–14.

(3) Meruelo, D.; Lavie, G.; Lavie, D. *Proc. Natl. Acad. Sci. U.S.A.* **1988**, *85*, 5230–5234.

(4) Kraus, G. A.; Pratt, D.; Tøsseberg, J.; Carpenter, S. *Biochem. Biophys. Res. Comm.* **1990**, *172*, 149–153.

(5) Lavie, G.; Mazur, Y.; Lavie, D.; Levin, B.; Ittah, Y.; Meruelo, D. *Aids: Anti-HIV Agents Therapies, and Vaccines* **1990**, *616*, 556–562.

(6) Lenard, J.; Rabson, A.; Vanderloef, R.; *Proc. Natl. Acad. Sci. U.S.A.* **1993**, *90*, 158–162.

(7) Takahashi, I.; Nakanishi, S.; Kobayashi, E.; Nakano, H.; Suzuki, K.; Tamaoki, T. *Biochem. Biophys. Res. Commun.* **1989**, *165*, 1207–1212.

(8) Andreoni, A.; Colasanti, A.; Colasanti, P.; Mastrocinque, M.; Riccio, P.; Roberti, G. *Photochem. Photobiol.* **1994**, *59*, 529–533.

(9) Couldwell, W. T.; Gopalakrishna, R.; Hinton, D. R.; He, S.; Weiss, M. H.; Law, R. E.; Apuzzo, M. L. *J. Neurosurgery* **1994**, *35*, 705–710.

(10) Carpenter, S.; Kraus, G. A. *Photochem. Photobiol.* **1991**, *53*, 169–174.

(11) Lavie, G.; Valentine, F.; Levin, B.; Mazur, Y.; Gallo, G.; Lavie, D.; Weiner, D.; Meruelo, D. *Proc. Natl. Acad. Sci. U.S.A.* **1989**, *86*, 5963–5967.

(12) Okpanyi, S. N.; Weischer, M. L. *Arzneimittel-Forschung* **1987**, *37*, 10–13.

(13) Utsumi, T.; Okuma, M.; Utsumi, T.; Kanno, T.; Yasuda, T.; Kobuchi, H.; Horton, A. A.; Utsumi, K. *Arch. Biochem. Biophys.* **1995**, *316*, 493–497.

(14) De Witte, P.; Agostinis, P.; Van Lint, J.; Merlevede, W.; Vandenhede, J. R. *Biochem. Pharmacol.* **1993**, *46*, 1929–1936.

(15) Thomas, C.; MacGill, R. S.; Miller, G. C.; Pardini, R. S. *Photochem. Photobiol.* **1992**, *55*, 47–53.

(16) Bouirig, H.; Eloy, D.; Jardon, P. *J. Chim. Phys.* **1992**, *89*, 1391–1411.

(17) Bouirig, H.; Eloy, D.; Jardon, P. *J. Chim. Phys.* **1993**, *90*, 2021–2038.

(18) Yamazaki, T.; Ohta, N.; Yamazaki, I.; Song, P. S. *J. Phys. Chem.* **1993**, *97*, 7870–7885.

(19) Gai, F.; Fehr, M. J.; Petrich, J. W. *J. Am. Chem. Soc.* **1993**, *115*, 3384–3385.

(20) Gai, F.; Fehr, M. J.; Petrich, J. W. *J. Phys. Chem.* **1994**, *98*, 5784–5795.

(21) Gai, F.; Fehr, M. J.; Petrich, J. W. *J. Phys. Chem.* **1994**, *98*, 8352–8358.

(22) Carpenter, S.; Fehr, M. J.; Kraus, G. A.; Petrich, J. W. *Proc. Natl. Acad. Sci. U.S.A.* **1994**, *91*, 12273–12277.

tization mechanism is the most widely reported, other observations lead to establish that oxygen is not always required for virucidal²⁶ and antitumoral⁹ activities of hypericin.

(ii) Others studies suggest that the virucidal activity may be due to complex mechanisms involving the superoxide anion and hypericinium ion, implicating a type I radical mechanism.^{27–29}

(iii) Finally, a recent publication²² suggests that an alternative origin for the photoinduced virucidal activity of hypericin may involve its ability to produce a photogenerated pH drop through an intramolecular proton transfer in the excited state of the molecule, which is likely to precede solvent acidification. Actually, a rapid (6–12 ps) proton transfer has been observed in the excited state of hypericin from one hydroxyl group to the adjacent carbonyl group,^{19–21} and a light-induced pH drop has been recently observed inside phosphatidylcholine vesicles during steady state illumination of a hypericin containing solution.³⁰ These authors suggest that a deprotonation process might result from hypericin excited triplet state, without excluding the possibility that the singlet excited state could provide protons as well. This would explain the light-dependent pH decrease which has been previously observed for the closely related stentorin chromophore from *S. coeruleus*.^{2,31} Possible mechanism, for the primary photoreaction, involving electron transfer coupled with proton transfer has also been proposed to account for this pH decrease.³²

In this study, using Snarf-1-AM as a specific fluorescent pH probe,³³ we have performed confocal laser microspectrofluorometric experiments in order to monitor possible intracellular local pH changes induced under photoexcitation of hypericin in single living cells.

Experimental Section

Chemicals. Hypericin was obtained from Roth Co. (Karlsruhe, Germany). Stock solutions were prepared in DMSO and stored in the dark at –20 °C. The pH probe Snarf-1-AM was purchased from Molecular Probes (Eugene, OR). Valinomycin and nigericin were purchased from Sigma Chemical Co. (St. Louis, MO).

Cell Culture. 3T3 mouse fibroblast cells were cultured as monolayers (25 cm² flask) at 37 °C in a humidified 5% CO₂ atmosphere, in RPMI 1640 medium supplemented with 10% foetal calf serum, 2 mM L-glutamine, streptomycin (0.1 mg/mL), and penicillin (100 U/ml), all from Boehringer (France). Cells were subcultured in 35 mm diameter Petri dishes for 48 h before microspectrofluorometric analysis. Hypericin (0.3 mM stock solution in DMSO) was then added to the culture medium to a final concentration of 10^{–6} M (0.3% DMSO) for 1 h before fluorescence measurements.

Microspectrofluorimetry. The experimental set-up is extensively described in supporting information.

Intracellular pH Determination. Intracellular pH of single cells has been monitored by the fluorescent pH indicator Snarf-1-AM.³³ Its

(23) Racinet, H.; Jardon, P.; Gautron, R. *J. Chim. Phys.* **1988**, *85*, 971–977.

(24) Jardon, P.; Lazortchak, N.; Gautron, R. *J. Chim. Phys.* **1987**, *84*, 1143–1145.

(25) Thomas, C.; Pardini, R. S. *Photochem. Photobiol.* **1992**, *55*, 831–837.

(26) Fehr, M. J.; Carpenter, S.; Petrich, J. W. *Bioorg. Med. Chem. Lett.* **1994**, *4*, 1339–1344.

(27) Weiner, L.; Mazur, Y. *J. Chem. Soc., Perkins Trans.* **1992**, *2*, 1439–1442.

(28) Redepenning, J.; Tao, N. *Photochem. Photobiol.* **1993**, *58*, 532–535.

(29) Diwu, Z.; Lowen, J. W. *Free Radical Biol. Med.* **1993**, *14*, 209–215.

(30) Fehr, M. J.; Mc Closkey, A.; Petrich, J. W. *J. Am. Chem. Soc.* **1995**, *117*, 1833–1836.

(31) Song, P. S.; Walker, E. B.; Auerbach, R. A.; Robinson, G. W. *Biophys. J.* **1981**, *35*, 551–555.

(32) Dai, R.; Yamazaki, T.; Yamazaki, I.; Song, P. S. *Biochim. Biophys. Acta* **1995**, *1231*, 58–68.

(33) Seksek, O.; Toulmé, N. H.; Sureau, F.; Bolard, J. *J. Anal. Biochem.* **1991**, *193*, 49–54.

emission spectrum exhibit two pH sensitive bands, protonated and unprotonated forms peaking at 590 and 635 nm, respectively. Its pK is about 7.4, which allows pH changes in the 6.3–8.6 range to be determined from intensity ratio measurements $R = I_f(635)/I_f(590)$. Cells were loaded with the fluorescent probes as follows: they were incubated in culture medium for 20 min at 37 °C, 5% CO₂, with 10 μM Snarf-1-AM from a 1 mM stock solution in DMSO. After loading, cells were washed and suspended in culture medium supplemented with 25 mM HEPES at pH 7.4 before MSF measurements. An in vivo calibration curve of R versus intracellular pH was first performed according to the method developed by Thomas.³⁴ Briefly, after incubation with the fluorescent probe, cells were washed and suspended in a buffer containing 10 mM Hepes, 130 mM KCl, 20 mM NaCl, 5 mM dextrose, 1mM CaCl₂, 1 mM KH₂PO₄, 0.5 mM MgSO₄ (Hepes saline buffer) at various pH values obtained by addition of small amounts of 0.1 M solutions of KOH and HCl. The pH changes of the external buffer of the cell were followed with a Tacussel Isis 20000 pH-meter. Addition of nigericin (1 μg/mL) and valinomycin (5 μM) allowed an exchange of K⁺ for H⁺ which resulted in a rapid equilibration of external and internal pH. In the pH range studied (6–8), cell viability was not significantly affected.

Results

The fluorescent pH indicator Snarf-1-AM³³ was chosen for pH measurements since it permits the same 514.5 nm laser line to be used for both hypericin photosensitization and probe excitation. Thus, local pH values determined from Snarf-1 fluorescence features actually correspond to instantaneous pH values induced by hypericin, during the time of illumination, in the subcellular microvolume (about 1 μm³) excited by the laser beam in the confocal mode. Consequently, it can be considered that photoinduced modifications of intracellular pH are only weakly balanced by the high buffering capability of the cells during measurements.

Classical fluorescence ratio imaging experiments would not be adequate for such measurements, since the fluorescence spectrum of hypericin strongly overlaps Snarf-1 fluorescence spectrum. To circumvent this problem, spectral analysis of the intracellular fluorescence may be performed by using microspectrofluorometric measurements.^{35,36} Actual fluorescence intensity ratios R , needed for local pH evaluation, were calculated after spectral decomposition of experimental signals by using previously recorded model spectra of hypericin and unprotonated and protonated forms of Snarf-1.

However, it has not been possible to obtain intracellular fluorescence spectra of totally protonated and/or unprotonated forms of Snarf-1 even after equilibration of intracellular pH with acidic (pH < 6) or basic (pH > 8.5) external buffers. This could be explained by the fact that a significant fraction of the dye remains specifically bound to cellular proteins, as previously reported.³³

The decomposition process can easily be performed by using any two distinct intracellular spectra of Snarf-1 (i.e., F_{sn1} , F_{sn2}), which present different R ratios. Thus any of the experimental spectra (F_{exp}) can be expressed as a linear combination of three model spectra:

$$F_{exp} = aF_{sn1} + bF_{sn2} + cF_{hyp}$$

F_{hyp} being the pure intracellular fluorescence model spectrum of hypericin.

The actual ratio $R = I_f(635)/I_f(590)$ is then calculated from the $aF_{sn1} + bF_{sn2}$ component. Validity of the spectral decom-

(34) Thomas, J. A.; Buschbaum, R. N.; Zimniak, A.; Racker, E.; *Biochemistry* **1979**, *18*, 2210–2218.

(35) Sureau, F.; Chinsky, L.; Duquesne, M.; Laigle, A.; Turpin, P. Y.; Amirand, C.; Ballini, J. P.; Vigny, P. *Eur. Biophys. J.* **1990**, *18*, 301–307.

(36) Sureau, F.; Moreau, F.; Millot, J. M.; Manfait, M.; Allard, B.; Aubard, J.; Schwaller, M. A. *Biophys. J.* **1993**, *65*, 1767–1774.

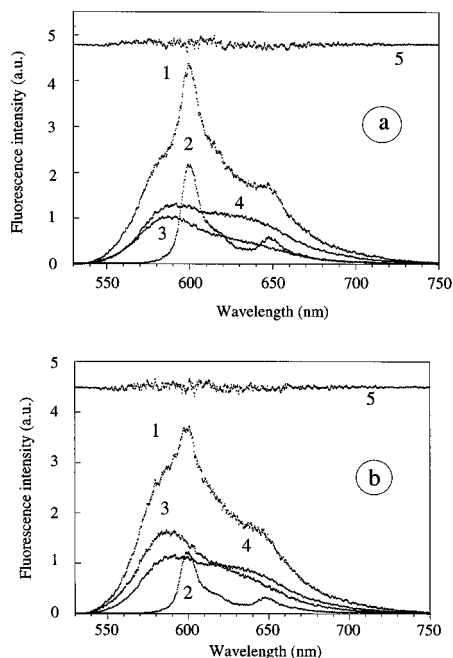


Figure 2. Resolution of experimental intracellular spectra (1), recorded after 1 s (a) and 90 s (b) of irradiation, by using model spectra of hypericin (2) and Snarf-1 at two distinct pHs (3, 4). Curve 5 present the residual weight obtained after subtraction of the calculated spectrum to the experimental spectrum. $\lambda_{exc} = 514.5$ nm, laser power = $0.1 \mu\text{W}$, acquisition time = 1s/spectrum.

position procedure is confirmed by comparison of experimental and recalculated spectra (trace of the residual weight shown on Figure 2 actually corresponds to their difference).

The relative contribution of the two emission bands of Snarf-1 obtained for hypericin treated cells after 90 s of $0.1 \mu\text{W}$ irradiation (Figure 2b, curves 3 and 4) is different from that observed after 1 s of irradiation under same power (Figure 2a).

Figure 4a presents a typical time evolution of the fluorescence intensity ratio R of these two bands, obtained on single cells, as a function of the time of irradiation of control and hypericin treated cells. While R appears to be practically independent of the time of irradiation for the control cell ($R = 0.62 \pm 0.010$), it decreases from an initial value of 0.615 ± 0.010 to a final value of 0.555 ± 0.010 for a cell incubated with hypericin. According to the calibration curve (Figure 3) these ratios correspond to an intracellular pH of 7.3 ± 0.05 for the control cell (in agreement with previously reported data³⁷) and to an intracellular pH value going from 7.23 ± 0.05 to 6.98 ± 0.02 for hypericin treated cell. Moreover, along with this pH decrease, a simultaneous linear photodegradation process of hypericin has been observed, as shown by the time evolution of its intracellular fluorescence intensity (Figure 4b).

Distributions of the intracellular pH values obtained in 3T3 cell populations after 90 s of irradiation with $0.1 \mu\text{W}$ of illumination are presented in Figure 5. Mean intracellular pH values of 7.25 ± 0.2 and 6.85 ± 0.2 were respectively obtained for control and hypericin treated cells (Figure 5a,b, respectively), external pH being of 7.4 ± 0.05 .

Discussion

Hypericin is a powerful photosensitizer that displays potential pharmacological applications including virucidal activity^{3,6,38} and antitumor properties.^{8,9} The relative importance of singlet oxygen in the toxicity of hypericin toward HIV and related

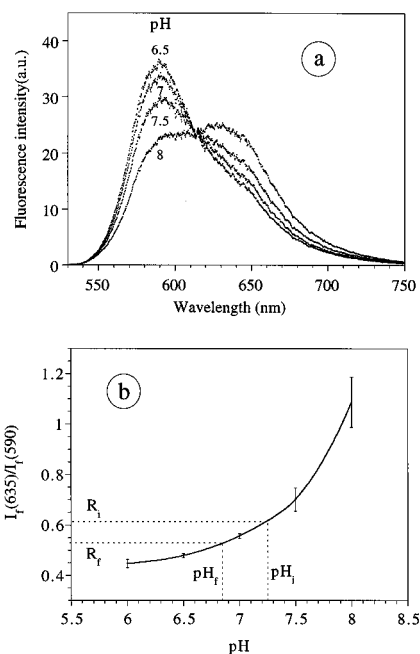


Figure 3. Microspectrofluorometric analysis of Snarf-1-AM loaded 3T3 cells. (a) Fluorescence emission spectra for various intracellular pH (calibration of intracellular pH was obtained as described in materials and methods). (b) $R = (\text{fluorescence emission intensity at } 635 \text{ nm})/(\text{fluorescence emission intensity at } 590 \text{ nm})$ plotted versus pH. For each pH values, number of cells = 20. R_i , pH_i and R_f , pH_f correspond to initial (1 s) and final (90 s) values of R and corresponding pH, respectively, on illumination of hypericin-treated cells (see Figure 4).

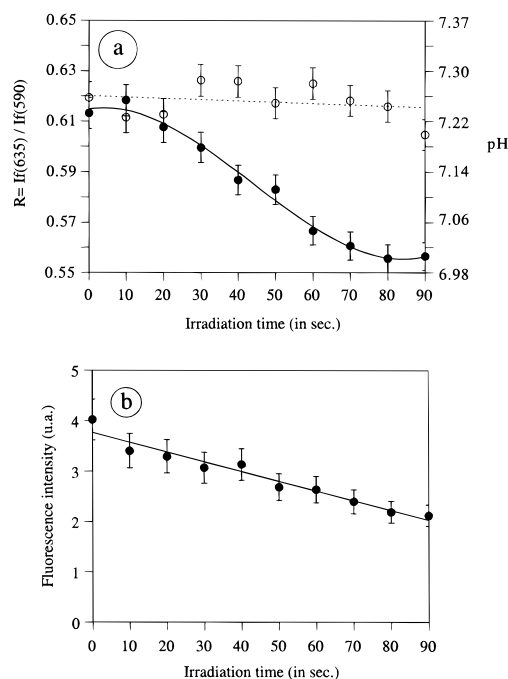


Figure 4. Typical time evolution of the intracellular pH (a) and of the intracellular fluorescence intensity of hypericin (b) under continuous laser irradiation: (○) control cells, (●) cells after 30 min of incubation in $1 \mu\text{M}$ hypericin. Error bars represent the accuracy of determination of R and corresponding pH values.

viruses has been recently questioned,^{19,26} and the production of a photogenerated pH drop has been suggested as an alternative origin for its photoinduced virucidal activity.²²

In the present work, confocal laser microspectrofluorometric analysis has been used to monitor intracellular pH during photosensitization of cells by hypericin. A mean pH decrease of 0.4 unit has been observed in the laser irradiated subcellular

(37) Seksek, O.; Bolard, J. *J. Cell Science* **1996**, *109*, 257–262.

(38) Lopez-Bazzocchi, I.; Hudson, J. B.; Towers, G. H. N. *Photochem. Photobiol.* **1991**, *54*, 95–98.

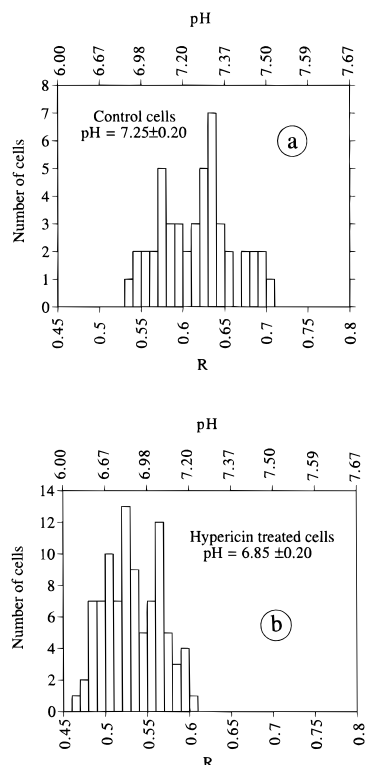


Figure 5. Distributions of intracellular pH values in 3T3 cells in Hepes saline buffer (pH 7.4) determined after 90 s of irradiation: (a) untreated control cells ($n = 77$) and (b) hypericin treated cells ($n = 93$). $\lambda_{\text{exc}} = 514.5$ nm, excitation power = $0.1 \mu\text{W}$, acquisition time = 1 s/spectrum.

microvolume (a few micrometers³) as shown in Figure 5. However, under $0.1 \mu\text{W}$ of excitation power this pH decrease is not linear as a function of the time of exposure (Figure 4a). The sigmoidal shape of the kinetic profile is assumed to result from two competitive processes: (i) acidification through proton release,³⁰ and (ii) neutralization of this acidification due to the high buffering capability of the cells which was previously reported to be *ca.* 40 mM for mammalian cells.³⁹ Apparently the 0.4 pH unit decrease observed under this laser irradiation would imply a very high intracellular concentration of hypericin, unless each of these molecules is producing hundreds of protons. Taking into account that (i) intracellular concentration of Snarf-1 has previously been calculated as high as 200 ± 50 mM under same experimental staining conditions³³ and (ii) the efficiencies of emission detection of both molecules, estimated from the $\epsilon_{514}^* \Phi_f$ product of extinction coefficients and fluorescence quantum yields ($\epsilon_{514} \approx 26\,000$ and $6\,000$, $\Phi_f \approx 0.05$ and 0.25 for Snarf-1⁴⁰ and hypericin,¹⁸ respectively), are roughly the same, it is possible that hypericin, which is not soluble in water, is also highly concentrated in cells, i.e., *ca.* 200 μM , as suggested by its fluorescence intensity which is of the same order of magnitude as that of Snarf-1 (Figure 2).

Moreover, the regulation of the intracellular pH through the Na^+/H^+ antiport⁴¹ of the plasma membrane might be inactivated since hypericin is a potent inhibitor of PKC^{7,13} which is involved in the regulation of the Na^+/H^+ activity.

Finally, the same range of pH drop can be observed either after 1 s of irradiation with $1 \mu\text{W}$ (data not shown) or after 90 s irradiation with $0.1 \mu\text{W}$ (Figure 4a): thus the intracellular

hypericin induced pH modification clearly appears to be light-dose dependent.

A possible artifact involving an energy transfer between hypericin and Snarf-1 can be discarded since (i) a reabsorption of hypericin fluorescence emission, which overlaps the absorption band of the unprotonated form of Snarf-1 (not shown), would result in an increase of the *R* ratio and (ii) a reabsorption of the fluorescence component arising from protonated Snarf-1 form, which overlaps the absorption spectrum of hypericin (not shown), would also result in an increase of the *R* ratio.

Finally, during the time course of intracellular acidification, a decrease of the overall fluorescence emission of hypericin has been observed (Figure 4b). To interpret this, one has to recall previous studies showing that protonation of one or both of the carbonyl groups of hypericin, achieved through an intramolecular proton transfer in its excited state, is required to promote its fluorescence emission.^{20,21} Consequently, a non-reversible proton release from the excited state of the chromophore to the bulk progressively precludes the fluorescence emission and can be considered as the first step of formation of a non fluorescent photoproduct of the molecule.

Conclusions

Intracellular pH changes, as large as 0.4 pH unit, can be considered as a possible mechanism responsible for the photosensitizing properties of hypericin. Several investigations have demonstrated the critical role of pH in the replication cycle of certain enveloped viruses by regulating uncoating.^{42,43} Intracellular acidification down to 6.8 has also been reported to precede apoptosis in various cell lines^{44–47} and can be involved in the hypericin induced apoptosis observed in glioma cell lines.⁹ This intracellular acidification can also be directly involved in the photoinduced antitumoral activity of hypericin which has been previously observed on EMT6 mouse mammary carcinoma²⁵ or human glioma⁹ cell lines. This assumption is supported by other studies on same EMT6 and glioma cell lines, which have shown that a decrease of intracellular pH constitutes a potent alternative for antitumor therapy.^{48–50}

Present results support the assumption that, besides the classical type-I and type-II photosensitization mechanisms, photoinduced pH variations have to be considered to account for some of the pharmacological properties of hypericin, in particular those which were reported not to be oxygen-dependent.

Acknowledgment. P. Miskovsky currently is an Invited Professor at Pierre et Marie Curie University, Paris, France.

Supporting Information Available: Experimental set-up of microspectrofluorimetry (1 page). See any current masthead page for ordering and Internet access instructions.

JA961783K

(42) Zhirmov, O. P. *Virology* **1990**, *176*, 274–279.

(43) Pinto, L. H.; Holsinger, L. J.; Lamb, R. A. *Cell* **1992**, *69*, 517–528.

(44) Barry, M. A.; Reynold, J. E.; Eastman, A. *Cancer Res.* **1993**, *53*, 2349–2357.

(45) Zhang, W.; Lawa, R. E.; Hinton, D. R.; Su, Y.; Couldwell, W. T. *Cancer Lett.* **1995**, *96*, 31–35.

(46) Li, J.; Eastman, A. *J. Biol. Chem.* **1995**, *270*, 3203–3211.

(47) Gottlieb, R. A.; Nordberg, J.; Skowronski E.; Babior, B. M. *Proc. Natl. Acad. Sci. U.S.A.* **1996**, *93*, 654–658.

(48) Newell, K. J.; Tannock, I. F. *Cancer Res.* **1989**, *49*, 4447–4482.

(49) Newell, K. J.; Wood, P.; Stratford, I.; Tannock, I. *Br. J. Cancer* **1992**, *66*, 311–317.

(50) Miccoli, L.; Oudard, S.; Sureau, F.; Poirson, F.; Dutrillaux, B.; Poupon, M.F. *Biochem J.* **1995**, *313*, 957–962.

(39) Roos, A.; Boron, W. F. *Physiol. Rev.* **1981**, *61*, 296–434.

(40) Whitaker, J. E.; Haugland, R. P.; Prendergast, F. G. *Anal. Biochem.* **1991**, *194*, 330–344.

(41) Grinstein, S.; Rotin, D.; Mason, M. J. *Biochem. Biophys. Acta* **1989**, *988*, 73–97.